Lipid-Lowering Drug, Fenofibrate Combined with si-HOTAIR Can Effectively Inhibit the Proliferation of Gliomas

Wei Zhu
Shandong University
Hongyang Zhao
Shandong University
Fenfen Xu
Shandong University
Bin Huang
Shandong University
Xiaojing Dai
The University of Texas MD Anderson Cancer Center
Jikui Sun
Nankai University
Alphonce Nyalali
Shandong University
Kailiang Zhang (Kailiang-Zhang@email.sdu.edu.cn)
Shandong University
Shilei Ni
Shandong University

Research Article

Keywords: Glioblastoma, Fenofibrate, HOTAIR, PPARA, Therapy

Posted Date: December 3rd, 2020

DOI: https://doi.org/10.21203/rs.3.rs-111977/v1

Abstract

Background: Fenofibrate is a fibric acid derivative known to have a lipid-lowering effect. Although fenofibrate-induced peroxisome proliferator-activated receptor alpha (PPARα) transcription activation has been shown to play an important role in the malignant progression of gliomas, the underlying mechanisms are poorly understood.

Methods: In this study, we analyzed the TCGA database and found that there is a significant negative correlation between long non-coding RNA (lncRNA) HOTAIR and PPARα. Then we explored the molecular mechanism of lncRNA HOTAIR regulating PPARα from the level of *in vitro* cell lines and the level of nude mouse glioma model *in vivo*, and explored the effect of combined application of HOTAIR knocking down and fenofibrate treatment on glioma invasion.

Results: For the first time, it was shown that after knocking down the expression of HOTAIR in gliomas, the expression of PPARα was significantly up-regulated, and the invasion and proliferation ability of gliomas were obviously inhibited. Then, glioma cells were treated with both PPARα agonist, fenofibrate and si-HOTAIR; results showed that proliferation and invasion of glioma cells were significantly inhibited.

Conclusions: Our results suggest that HOTAIR can negatively regulate the expression of PPARα, and the combination of fenofibrate and si-HOTAIR treatment can significantly inhibit the progression of gliomas. This introduces new ideas for the treatment of gliomas.

Background

The incidence of primary brain tumors in the world is about 7/100,000 per year. It accounts for about 2% of primary tumors that occur before the age of 70, and 7% of all cancer deaths. Glioma is the most common primary brain tumor, accounting for about 80% of all primary malignant brain tumors; and glioblastoma is the most common type of gliomas accounting for more than 50% of all brain glial tumors, and is the most aggressive among all gliomas (WHO grade IV). Glioblastoma (GBM) is characterized by uncontrolled cell proliferation, diffuse infiltration, necrosis tendency, strong angiogenesis, strong resistance to apoptosis, and genomic instability. As reflected in the old name "multiforme", GBM exhibits significant intratumoral heterogeneity at the cytopathology, transcription and genomic levels [1]. These characteristics make GBM one of the most difficult malignancies to analyze and treat. Despite the implementation of intensive treatment strategies and supportive care, the median survival of GBM has remained 12 months in the past decade [2]. Therefore, continued in-depth study of the pathogenesis of GBM and the development of new targeted therapy methods based on its histomorphological, molecular and genomic characteristics remain crucial scientific research topics in the field of neurosurgical oncology.

In recent years, non-coding RNAs (ncRNAs) have been shown to be involved in the malignant progression of tumors as well as playing an important role in tumor proliferation, cell cycle progression, angiogenesis, apoptosis and invasion [3, 4]. This type of regulatory RNAs that do not encode proteins mainly includes

microRNA, lncRNA, nucleolar small RNA, and interfering RNA (siRNA), etc. Among these RNAs, the most studied are miRNAs and lncRNAs. MiRNA regulates gene expression at the post-transcription level by targeting the 3'-untranslated region (3' UTR) of specific messenger RNAs (mRNA). LncRNA has been shown to be related to chromosome modification, transcription and post-transcriptional regulation [5-7].

Peroxisome proliferator-activated receptors (PPARs) are members of nuclear receptor superfamily involved in fatty acid oxidation and, glucose and lipid metabolism. They are composed of three subtypes: PPARα, PPARβ, and PPARγ. PPARα participates in lipid metabolism and plays an important role in regulating cell growth, differentiation, and apoptosis. Recent research results suggest that PPARα is involved in the malignant progression of tumors [8]. Fenofibrate, as a PPARα agonist, can inhibit the growth of gliomas in animal models of gliomas [9]. In addition, experimental results show that non-coding RNA is involved in the regulation of PPARα signaling pathway [10]. However, the specific control mechanism remains to be further explored.

This study intended to explore the mechanism of lncRNA HOTAIR in regulating PPARα, in-depth description of the role of HOTAIR in the malignant progression of glioma by *in vivo* animal experiments and *in vitro* cell line experiments and, to verify the therapeutic effect of the combination of si-HOTAIR and PPARα agonist fenofibrate on glioma cells. This study provides an experimental basis for us to understand the pathogenesis of GBM, and also new ideas for molecular treatment of gliomas in clinical settings.

Methods

Patient samples

A total of 702 glioma samples from TCGA (The Cancer Genome Atlas) were used in this study, including 530 low-grade gliomas and 172 glioblastomas. The data related to the changes in the binding of EZH2 and H3K27me3 proteins in the PPARA promoter region in glioma samples of different grades were obtained from the GEO database (GSE126396).

Cell culture

The human GBM cell lines U87 and U251 were purchased from ATCC (Manassas, Virginia, USA) in August 2015. After obtaining the U87 and U251 cell lines, they were immediately proliferated and frozen in liquid nitrogen for subsequent studies. U251 cells were cultured in complete MEM (Gibco) medium, while U87 cells were cultured in DMEM (Gibco) medium containing 10% FBS at 37 °C in 5% CO_2 incubation. With the exception of *in vivo* cultures, all glioblastoma cells were maintained for less than eight generations.

GO analysis, survival curve plot and heat map

GO analysis was performed using the Cluster Profiler [11] R package. A survival curve plot was performed using the survminer (https://github.com/kassambara/survminer/issues) R package. Heat map plots were built using cluster 3.0 (Stanford University).

Western blot analysis

Protein was extracted from cells that were seeded without FBS and were treated with drugs following a concentration gradient for 24 h. Equal amounts of total protein (nucleoprotein) per lane were separated using 10% or 15% SDS-polyacrylamide gel electrophoresis and then transferred to a PVDF membrane. The membrane was blocked in 5% skim milk for 1 h and then incubated with primary antibody for 2 h. The primary antibodies used were anti-H3K27me3 (Cell Signaling Technology, USA), anti-PPARα (Proteintech) and anti-GAPDH (Proteintech). Detection of protein bands was performed using a Super Signal protein detection kit (Pierce, USA). The band densities of specific proteins were quantified after normalization to the density of the GAPDH band.

Analysis of wound healing and perforation migration

U87 and U251 cells were infected with control or lentivirus containing si-HOTAIR segment, and then fenofibrate (Sigma-Aldrich) was introduced to treat the cells at a concentration of 100 μM or not. Cells in each group (control, si-HOTAIR, si-HOTAIR+fenofibrate) were seeded into 6-well plates. After 24 hours, a 200 μl sterile pipette tip was used to evenly scrape a single layer cells. The cell debris was removed by washing with PBS (phosphate buffered saline). Then, the cells were incubated with serum-free medium under normal conditions. Photos were taken at 0 and 48 hours after scratching. The wound area was evaluated by ImageJ, and the percentage of wound healing was calculated as follows: (0 hour wound area-48 hour wound area) / 0 hour wound area × 100.

For the *in vitro* migration assays, U87-control, U87-si-HOTAIR, U87-si-HOTAIR+fenofibrate, U251-control, U251-si-HOTAIR, U251- si-HOTAIR+fenofibrate cells were seeded into the upper culture chamber of a 24-well transwell plate. The medium in the upper chamber contained no serum, and the medium in the lower chamber contained 10% FBS. After incubation at 37 ℃ for 48 hours, non-migrating cells on the upper surface of the membrane were removed with a cotton swab. Cells that passed through the membrane were fixed with methanol, stained with crystal violet, and counted in 5 random fields under an optical microscope (100x magnification).

Colony formation test

After treated U87 and U251 cells with control, si-HOTAIR or si-HOTAIR+fenofibrate, they were inoculated into 6-well plates and incubated. After 14 days, the cells were fixed with 4% paraformaldehyde and stained with 0.1% crystal violet. We used a digital camera to capture pictures from different transfected colonies (more than 50 cells per clone).

Chromatin immunoprecipitation (ChIP) and ChIP-qPCR assays

ChIP assays were performed using a commercially available ChIP Assay Kit (Beyotime). The ChIP-qPCR primers used were as follows: Forward-1: AACCTTGGGAGCCCCAAAAA and reverse-1: GTGCAGAGTGGTCACGTACA; Forward-2: GAGCGTGGTTTCCCAGAAGA and reverse-2: TTTGGGGCTCCCAAGGTTTT; Forward-3: TACGTGACCACTCTGCACAC and reverse-3: CCTCCGGGCTCAAAGACATT; forward-4: TACGTGACCACTCTGCACAC and reverse-4: CCTCCGGGCTCAAAGACATT.

Nude mouse intracranial glioma model and *in vivo* bioluminescence imaging

BALB/c-A nude mice were purchased from the Animal Center of Cancer Institute of Chinese Academy of Medical Sciences (Beijing) and their care was in accordance with institution guidelines. Three to five weeks old mice were selected as the intracranial tumor model. U87 and U87-si-HOTAIR cells (5×10^5) were stereotactically injected into the right striatum of nude mice. Seven days after injection, 200 mg/kg of fenofibrate suspended in 5% sodium carboxymethylcellulose were given daily via intragastric administration in treatment group, while the equal volume of 5% sodium carboxymethylcellulose was administrated in the control group. The treatment lasted 21 days. The growth of intracranial tumors was monitored on days 7, 14, 21, and 28 using a bioluminescence imaging system.

Histopathology

The whole brains of the mice were harvested on day 28 after allogeneic glioma cells were implanted, fixed in 4% paraformaldehyde, and then embedded in paraffin, and cut into 15 μm thick coronal slices. The sections with the largest tumor area were stained with hematoxylin and eosin or were used for IHC staining. For the IHC analysis, we quantitatively scored the tissue sections according to the percentage of positive cells and staining intensity. We assigned the following proportion scores: 1 if 0–25% of the tumor cells showed positive staining, 2 if 26–50% of cells were stained, 3 if 51–75% stained, and 4 if 76–100% stained; we also divided different expression levels into four different groups (1 to 4) and scored them.

Results

There was a negative correlation between the expression of HOTAIR and PPARα in glioma

In order to verify the regulation mechanism of HOTAIR gene on the occurrence and progression of glioma, we heat-mapped about 2600 genes negatively related to HOTAIR expression. The results suggest that almost all genes are highly expressed in low-grade gliomas (Figure 1A), and the expression level decreases as the tumor grade increases. Further GO analysis of these genes showed that their biological processes are regulation of membrane potential, modulation of chemical synaptic transmission and, regulation of trans-synaptic signaling and synapse organization (Figure 1B).

We then analyzed the signal pathways enriched in these genes and found that there are mainly cAMP signaling pathway, AMPK signaling pathway and phosphatidylinositol signaling system (Figure 1B).

Most of these signaling pathways have been confirmed by scholars to be involved in the progression of tumors and different degrees of abnormal cell behaviors [12]. Excessive activation of phosphatidylinositol could lead to abnormal cell proliferation, abnormal endocytosis and exocytosis, abnormal cell metastasis and even tumor development [13]. AMP kinase promotes the bioenergy and tumor growth of glioblastoma [14].

AMPK pathway and PPARA are all involved in metabolic activities such as fatty acid oxidation and block of glycolysis and protein, nucleotide and fatty acid synthesis. We further examined the expression of HOTAIR and PPARα in gliomas. The results suggest that there is a significant negative correlation between them. The Pearson correlation coefficient was -0.32 (Figure 2A). By comparing the expression levels of HOTAIR and PPARα in low-grade gliomas and glioblastomas, it was found that the expression of HOTAIR in GBM was up-regulated, while PPARα had low expression state (Figure 2B). In the results of survival analysis, it was found that the high expression of HOTAIR indicated a poor prognosis, but the high expression of PPARA indicated a good survival prognosis (Figure 2C and D). These results indicate that there is a negative correlation between the expression of lncRNA HOTAIR and PPARα in gliomas, and it has a significance of indicating survival rate and clinical grade.

PPARA expression decreased in clinical samples of patients with high-grade glioma

Through survival analysis of GBM (WHO grade IV), we found that the low expression level of PPARA in the TCGA database was significantly associated with poor prognosis of patients (Figure 2D). To avoid the bias from the analysis of only mRNA expression data, we examined the PPARA protein levels of 21 different grades glioma samples by immunohistochemistry (IHC) staining (clinical information is listed in Supplementary Table 1). As shown in Figure 3A, we observed a significant decrease in PPARA protein levels in high-grade gliomas. Quantification of the staining (see Methods) revealed a strong association between the abundance of PPARA positive cells and lower tumor grade (Figure 3B). Therefore, the down-regulated expression level of PPARA is an indicator of the aggressiveness of malignant gliomas.

The expression level of HOTAIR enhanced the degree of H3K27me3 binding to the PPARA promoter

H3K27me3 is a histone modification related to transcription repression. HOTAIR can promote the formation of H3K27me3 through EZH2 protein, and then silence the transcriptional expression of genes and promote the malignant progression of glioma. Analysis of the GSE126396 database showed that there was a significant difference in the amount of H3K27me3 protein enrichment in the PPARA promoter region of glioma samples of different malignancies (Figure 4A). In order to investigate whether HOTAIR overexpression mediated PPARA promoter gene silencing, we analyzed the binding of HEK27me3 in the PPARA promoter region in control, HOTAIR and si-HOTAIR GBM cell lines by ChIP-PCR. The experimental results showed that the high expression of HOTAIR can promote the enrichment of H3K27me3 protein in the PPARA promoter region, while reducing the expression of HOTAIR in glioma cell lines can reduce the amount of binding (Figure 4B and C). RT-PCR, western blot and immunofluorescence experiments were used to analyze the expression of PPARA mRNA and protein in GBM cell lines of control, HOTAIR and si-HOTAIR. It was found that the expression of HOTAIR had a negative regulatory relationship with PPARA

(Figure 4D~F). Based on the above findings, we concluded that the ezh2-H3K27me3 pathway mediated by HOTAIR can silence the transcriptional expression of PPARA.

Low expression of HOTAIR and activation of PPARA pathway weakened the migration and colony-forming ability of U87 and U251 glioma cells

In order to study the role of HOTAIR in gliomas, we transfected U87 and U251 glioma cells with si-HOTAIR lentivirus. Transwell migration, wound healing and colony formation analyses were performed to examine the effect of HOTAIR on glioma cells migration and colony formation. As shown by our results, U87 and U251 cells with low expression of HOTAIR showed lower migration ability compared to control cells (Figure 5A, 5C and 5E). The statistical results also showed the same results (Figure 5B and 5D). In further experiments, we treated si-HOTAIR group glioma cell lines with fenofibrate（100 μM） and found that the cell migration and colony-formation ability were further decreased. These results indicate that the activation of the PPARA pathway can suppress the malignant phenotype of gliomas, and the combination of down-regulation of HOTAIR and activation of the PPARA pathway can more effectively inhibit the malignant progression of gliomas.

Reducing HOTAIR expression in glioma cells combined with fenofibrate treatment can effectively inhibit the growth of glioma xenografts

To investigate whether reducing HOTAIR expression combined with fenofibrate treatment will reduce the growth of glioma *in vivo*, nude mice were implanted intracranially with U87 cells infected with lentivirus containing si-HOTAIR segment or control lentivirus to form glioma xenografts. The si-HOTAIR group was randomly divided into control treatment and finofibrate treatment groups. Seven days after injection, 200 mg/kg of fenofibrate suspended in 5% sodium carboxymethylcellulose were given daily via intragastric administration in treatment group, while the equal volume of 5% sodium carboxymethylcellulose was administrated in the control group. The treatment lasted 21 days. On days 7, 14, 21, and 28 after implantation, the bioluminescence imaging of the three groups of NC, si-HOTAIR and combination therapy showed that the BLI signal intensity of the combination therapy group was significantly lower than that of the NC and si-HOTAIR groups (Figure 6A and B). The HE staining results were consistent with the bioimaging results (Figure 6A). Survival analysis showed that the prognosis of mice carrying the combined treatment group was significantly better (Figure 6C). Further immunohistochemical staining showed that, after reducing the HOTAIR expression of gliomas, the expression of PPARA protein was increased, and the CD34 and Ki67 protein expression of the combined treatment group was lower than that of the other two groups. These results indicated that in *in vivo* environment, reducing the expression of HOTAIR combined with fenofibrate treatment can effectively inhibit tumor proliferation and growth.

Discussion

GBM is the most common and deadly cancer of the central nervous system [15, 16]. However, current conventional treatments such as surgical resection, radiotherapy and chemotherapy do not significantly improve the patient's prognosis. Therefore, there is an urgent need to further study the molecular

pathways of gliomas development and explore feasible therapeutic options. Fenofibrate is an effective ligand for the peroxisome proliferator-activated receptor alpha (PPARα) and has historically been used to regulate glucose and lipid metabolism in the treatment of different forms of hyperlipidemia and hypercholesterolemia [17]. In recent years, fenofibrate has proved to have interesting anti-cancer effects [18-22].

HOTAIR regulates the expression of a variety of proteins through PRC2 [6, 23]. Studies by other scholars have confirmed that HOTAIR expression levels in tumors are higher than that in corresponding non-cancerous tissues. And its high expression predicted a poor prognosis [6, 23, 24]. In our previous studies, HOTAIR was considered not only an important marker of tumor classification and prognosis, but also an important marker of glioma molecular subtypes [5, 25, 26].

In this study, we analyzed the expression of HOTAIR based on the RNA expression database of 702 TGGA glioma patients, and analyzed the genes negatively related to HOTAIR expression using bioinformatics analyses and found many of these genes are involved in tumor formation (Figure 1A and B). Correlation analysis revealed that there was a significant negative correlation between HOTAIR and PPARα (Figure 2A) and, low expression of PPARα through survival analysis predicted a poor prognosis (Figure 2D). Through immunohistochemical staining of clinical samples, it was shown that with the increase of glioma grade, the expression level of PPARα will decrease significantly (Figure 3). Therefore, we predicted that HOTAIR can reduce the expression of PPARα through PRC2 protein, thereby promoting the malignant progression of glioma.

Through ChIP-PCR analysis, it was shown that after knocking down the expression of HOTAIR in glioblastoma, the binding of histone H3K27me3 in the promoter region of PPARα gene was significantly reduced (Figure 4A). And through quantitative PCR, western blot and immunofluorescence, it was found that the expression of PPARα increases significantly with the decrease of HOTAIR expression (Figure 4B ~ F). These results indicate that HOTAIR can increase the amount of H3K27me3 binding in the PPARα promoter region through PRC2, thereby silencing the transcriptional expression of PPARα. In further *in vitro* migration experiments, colony formation experiments and scratch experiments, it was found that after the combination of si-HOTAIR and fenofibrate treatment, the migration and colony-formation ability of glioma cells decreased significantly (Figure 5). The *in vivo* malignant glioma model also found that combined therapy can significantly reduce the rate of tumor cell proliferation, thereby extending the survival period of nude mice (Figure 6).

Conclusions

Our study not only explores the molecular mechanism of HOTAIR in regulating PPARα, but also verifies the therapeutic effect of the combined application of PPARα agonist fenofibrate and siRNA HOTAIR on glioma through *in vivo* animal experiments. This provides new ideas for comprehensive treatment of gliomas.

Abbreviations

HOTAIR: HOX transcript antisense RNA; **PPARα:** peroxisome proliferator-activated receptor alpha; **LncRNA:** long non-coding RNA; **GBM:** glioblastoma; **3' UTR:** 3'-untranslated region; **TCGA:** The Cancer Genome Atlas; **ChIP:** chromatin immunoprecipitation; **IHC:** immunohistochemical. PCR: polymerase chain reaction; PRC2: polycomb repressive complex 2; EZH2: enhancer of zeste homolog 2; AMPK: adenosine monophosphate-activated protein kinase; PVDF: polyvinylidene fluoride.

Declarations

Acknowledgements

None.

Authors' contributions

Wei Zhu, Data curation, Writing- Original draft preparation. **Hongyang Zhao, Fenfen Xu,** Software. **Bin Huang,** Visualization, Investigation. **Xiaojing Dai, Jikui Sun,** Software, Validation. **Alphonce M.K Nyalali,** Writing- Reviewing and Editing. **Kailiang Zhang, Shilei Ni,** Conceptualization, Methodology, Supervision.

Funding

This study was supported by National Natural Science Foundation of China (Grant No. 81874082, 81702470 and 81472353), Key Research and Development Plan of Shandong Province (Grant No. 2016GSF201014 and 2018GSF118094), Shandong Provincial Natural Science Foundation (Grant No. ZR2015HM074) and Jinan Science and Technology Development Plan (Grant No. 201821049).

Availability of data and materials

The datasets used and analyzed during the current study are available from the corresponding author on reasonable request.

Ethics approval and consent to participate

This study was approved by the Academic Committee of Qilu Hospital of Shandong University and was conducted in accordance with the principles expressed in the Helsinki Declaration. All datasets were obtained from published literature, so it can be confirmed that written informed consent was obtained.

Consent for publication

Not applicable.

Competing interests

The authors declare no competing interests.

Author details

[1]Department of Neurosurgery, Qilu Hospital, Cheeloo College of Medicine, Shandong University and Institute of Brain and Brain-Inspired Science, Shandong University, Jinan 250012, Shandong, China; [2]Key Laboratory of Brain Function Remodeling, Qilu Hospital of Shandong University, Jinan 250012, Shandong, China [3]Department of Neurosurgery, Yantai Yuhuangding Hospital, Cheeloo College of Medicine, Shandong University, Yantai, Shandong, 264000, China; [4]Department of Pediatrics, Jinan Central Hospital, Cheeloo College of Medicine, Shandong University, Jinan 250013, Shandong, China; [5]The Advanced Technology Genomics Core, The University of Texas MD Anderson Cancer Center, Houston 77030, TX, USA; [6]School of Medicine, Nankai University, 94 Weijin Road, Tianjin 300071, China; [7]Tianjin Cerebral Vascular and Neural Degenerative Disease Key Laboratory, Tianjin Neurosurgical Institute; Department of Neurosurgery, Tianjin Huanhu Hospital, Tianjin 300350, China; [8]Department of Orthopedics and Neurosurgery, Mbeya Zonal Referral Hospital and Mbeya University College of Medicine, University of Dar es Salaam, Mbeya Box419, Mbeya, Tanzania.

References

1. Rice T, Lachance DH, Molinaro AM, Eckel-Passow JE, Walsh KM, Barnholtz-Sloan J, Ostrom QT, Francis SS, Wiemels J, Jenkins RB *et al*: **Understanding inherited genetic risk of adult glioma - a review**. *Neurooncol Pract* 2016, **3**(1):10-16.
2. Furnari FB, Fenton T, Bachoo RM, Mukasa A, Stommel JM, Stegh A, Hahn WC, Ligon KL, Louis DN, Brennan C *et al*: **Malignant astrocytic glioma: genetics, biology, and paths to treatment**. *Genes Dev* 2007, **21**(21):2683-2710.
3. Anastasiadou E, Jacob LS, Slack FJ: **Non-coding RNA networks in cancer**. *Nat Rev Cancer* 2018, **18**(1):5-18.
4. Yang C, Wang L, Sun J, Zhou JH, Tan YL, Wang YF, You H, Wang QX, Kang CS: **Identification of long noncoding RNA HERC2P2 as a tumor suppressor in glioma**. *Carcinogenesis* 2019.
5. Huang K, Sun J, Yang C, Wang Y, Zhou B, Kang C, Han L, Wang Q: **HOTAIR upregulates an 18-gene cell cycle-related mRNA network in glioma**. *Int J Oncol* 2017.
6. Gupta RA, Shah N, Wang KC, Kim J, Horlings HM, Wong DJ, Tsai MC, Hung T, Argani P, Rinn JL *et al*: **Long non-coding RNA HOTAIR reprograms chromatin state to promote cancer metastasis**. *Nature* 2010, **464**(7291):1071-1076.
7. Zhang JX, Han L, Bao ZS, Wang YY, Chen LY, Yan W, Yu SZ, Pu PY, Liu N, You YP *et al*: **HOTAIR, a cell cycle-associated long noncoding RNA and a strong predictor of survival, is preferentially expressed in classical and mesenchymal glioma**. *Neuro-oncology* 2013, **15**(12):1595-1603.
8. Simula MP, Cannizzaro R, Canzonieri V, Pavan A, Maiero S, Toffoli G, De Re V: **PPAR signaling pathway and cancer-related proteins are involved in celiac disease-associated tissue damage**. *Molecular medicine (Cambridge, Mass)* 2010, **16**(5-6):199-209.

9. Piwowarczyk K, Wybieralska E, Baran J, Borowczyk J, Rybak P, Kosinska M, Wlodarczyk AJ, Michalik M, Siedlar M, Madeja Z *et al*: **Fenofibrate enhances barrier function of endothelial continuum within the metastatic niche of prostate cancer cells**. *Expert Opin Ther Targets* 2015, **19**(2):163-176.
10. Portius D, Sobolewski C, Foti M: **MicroRNAs-Dependent Regulation of PPARs in Metabolic Diseases and Cancers**. *PPAR Res* 2017, **2017**:7058424.
11. Yu G, Wang LG, Han Y, He QY: **clusterProfiler: an R package for comparing biological themes among gene clusters**. *Omics : a journal of integrative biology* 2012, **16**(5):284-287.
12. Jiang K, Yao G, Hu L, Yan Y, Liu J, Shi J, Chang Y, Zhang Y, Liang D, Shen D *et al*: **MOB2 suppresses GBM cell migration and invasion via regulation of FAK/Akt and cAMP/PKA signaling**. *Cell Death Dis* 2020, **11**(4):230.
13. Cheng CK, Fan Q-W, Weiss WA: **PI3K signaling in glioma–animal models and therapeutic challenges**. *Brain pathology (Zurich, Switzerland)* 2009, **19**(1):112-120.
14. Chhipa RR, Fan Q, Anderson J, Muraleedharan R, Huang Y, Ciraolo G, Chen X, Waclaw R, Chow LM, Khuchua Z *et al*: **AMP kinase promotes glioblastoma bioenergetics and tumour growth**. *Nat Cell Biol* 2018, **20**(7):823-835.
15. Siegel RL, Miller KD, Jemal A: **Cancer statistics, 2019**. *CA Cancer J Clin* 2019.
16. Louis DN, Perry A, Reifenberger G, von Deimling A, Figarella-Branger D, Cavenee WK, Ohgaki H, Wiestler OD, Kleihues P, Ellison DW: **The 2016 World Health Organization Classification of Tumors of the Central Nervous System: a summary**. *Acta Neuropathol* 2016, **131**(6):803-820.
17. Rosenson RS: **Fenofibrate: treatment of hyperlipidemia and beyond**. *Expert Rev Cardiovasc Ther* 2008, **6**(10):1319-1330.
18. Hu D, Su C, Jiang M, Shen Y, Shi A, Zhao F, Chen R, Shen Z, Bao J, Tang W: **Fenofibrate inhibited pancreatic cancer cells proliferation via activation of p53 mediated by upregulation of LncRNA MEG3**. *Biochemical and biophysical research communications* 2016, **471**(2):290-295.
19. Su C, Shi A, Cao G, Tao T, Chen R, Hu Z, Shen Z, Tao H, Cao B, Hu D *et al*: **Fenofibrate suppressed proliferation and migration of human neuroblastoma cells via oxidative stress dependent of TXNIP upregulation**. *Biochemical and biophysical research communications* 2015, **460**(4):983-988.
20. Panigrahy D, Kaipainen A, Huang S, Butterfield CE, Barnes CM, Fannon M, Laforme AM, Chaponis DM, Folkman J, Kieran MW: **PPARalpha agonist fenofibrate suppresses tumor growth through direct and indirect angiogenesis inhibition**. *Proc Natl Acad Sci U S A* 2008, **105**(3):985-990.
21. Grabacka M, Placha W, Plonka PM, Pajak S, Urbanska K, Laidler P, Slominski A: **Inhibition of melanoma metastases by fenofibrate**. *Arch Dermatol Res* 2004, **296**(2):54-58.
22. Zhang KL, Han L, Chen LY, Shi ZD, Yang M, Ren Y, Chen LC, Zhang JX, Pu PY, Kang CS: **Blockage of a miR-21/EGFR regulatory feedback loop augments anti-EGFR therapy in glioblastomas**. *Cancer Lett* 2014, **342**(1):139-149.
23. Kim K, Jutooru I, Chadalapaka G, Johnson G, Frank J, Burghardt R, Kim S, Safe S: **HOTAIR is a negative prognostic factor and exhibits pro-oncogenic activity in pancreatic cancer**. *Oncogene* 2013, **32**(13):1616-1625.

24. Kogo R, Shimamura T, Mimori K, Kawahara K, Imoto S, Sudo T, Tanaka F, Shibata K, Suzuki A, Komune S *et al*: **Long Noncoding RNA HOTAIR Regulates Polycomb-Dependent Chromatin Modification and Is Associated with Poor Prognosis in Colorectal Cancers**. *Cancer Research* 2011, **71**(20):6320-6326.
25. Wu L, Murat P, Matak-Vinkovic D, Murrell A, Balasubramanian S: **Binding interactions between long noncoding RNA HOTAIR and PRC2 proteins**. *Biochemistry* 2013, **52**(52):9519-9527.
26. Zhang K, Sun X, Zhou X, Han L, Chen L, Shi Z, Zhang A, Ye M, Wang Q, Liu C *et al*: **Long non-coding RNA HOTAIR promotes glioblastoma cell cycle progression in an EZH2 dependent manner**. *Oncotarget* 2015, **6**(1):537-546.

Figures

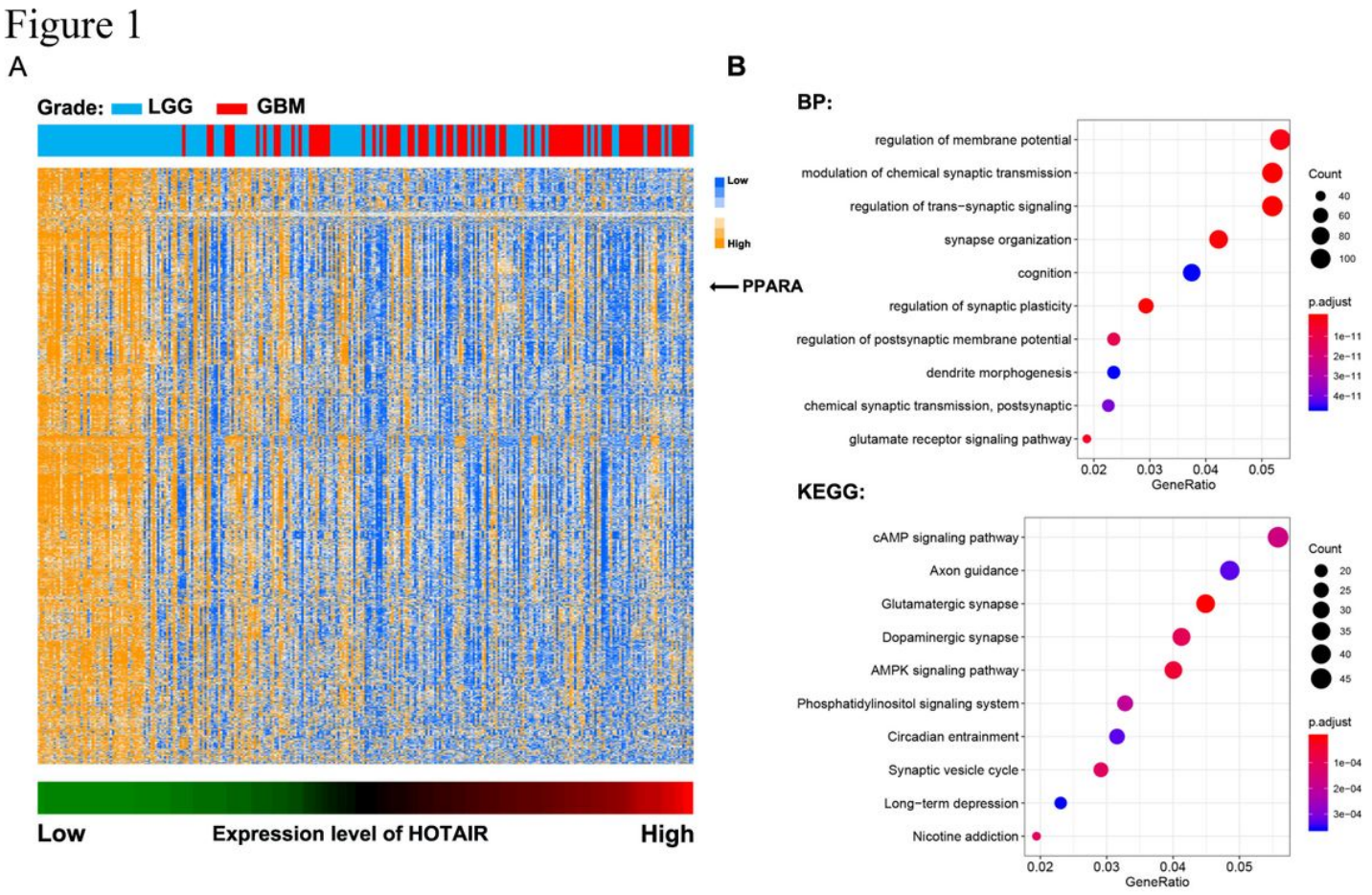

Figure 1

The expression of HOTAIR and PPARα in glioma has a negative correlation. A) Expression heat map of genes in the TCGA glioma database that are significantly negatively related to HOTAIR expression. The genes are arranged according to the changes in HOTAIR expression. B) GO analysis and KEGG analysis of genes negatively related to HOTAIR expression.

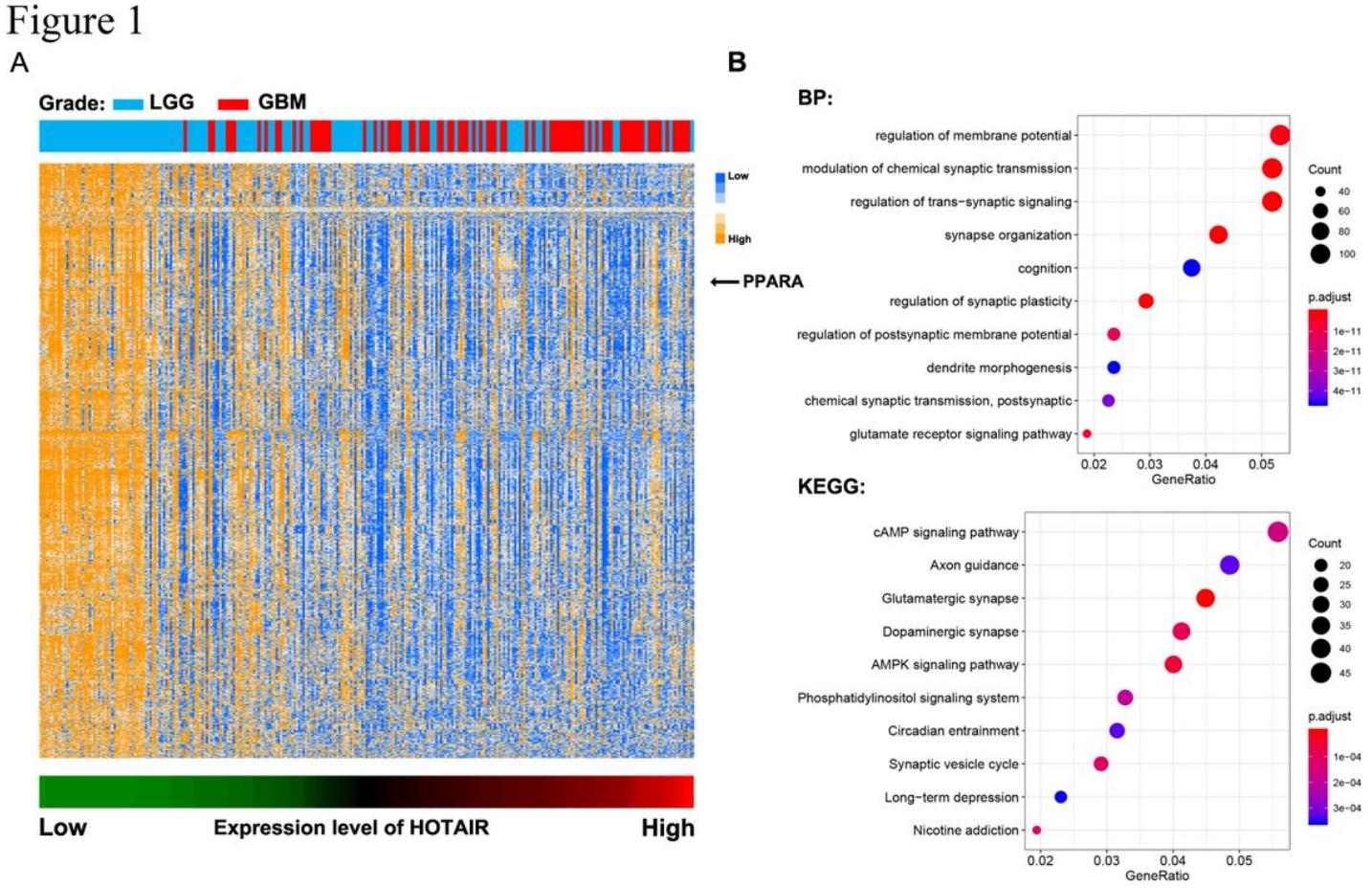

Figure 1

The expression of HOTAIR and PPARα in glioma has a negative correlation. A) Expression heat map of genes in the TCGA glioma database that are significantly negatively related to HOTAIR expression. The genes are arranged according to the changes in HOTAIR expression. B) GO analysis and KEGG analysis of genes negatively related to HOTAIR expression.

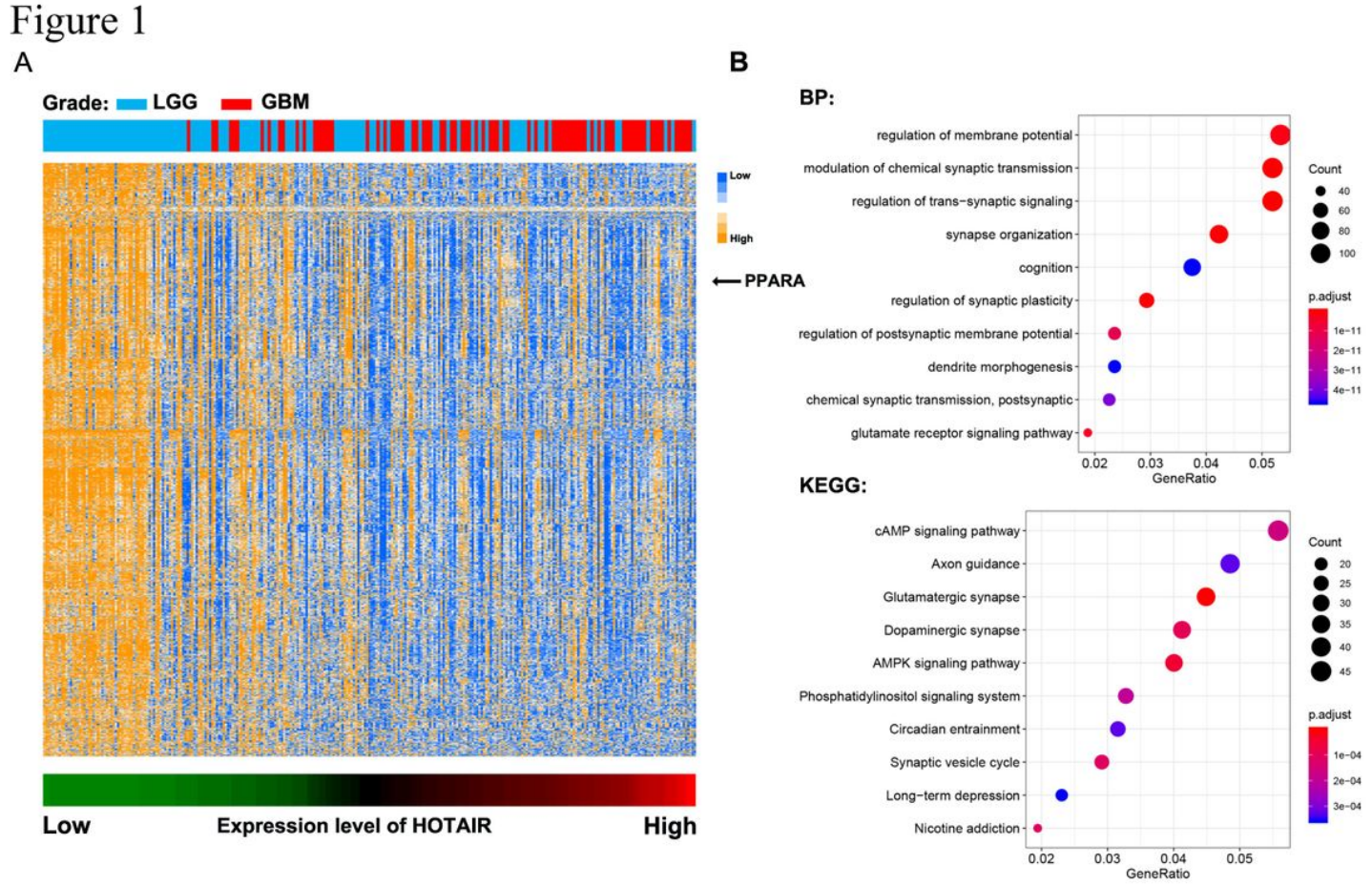

Figure 1

The expression of HOTAIR and PPARα in glioma has a negative correlation. A) Expression heat map of genes in the TCGA glioma database that are significantly negatively related to HOTAIR expression. The genes are arranged according to the changes in HOTAIR expression. B) GO analysis and KEGG analysis of genes negatively related to HOTAIR expression.

Figure 2

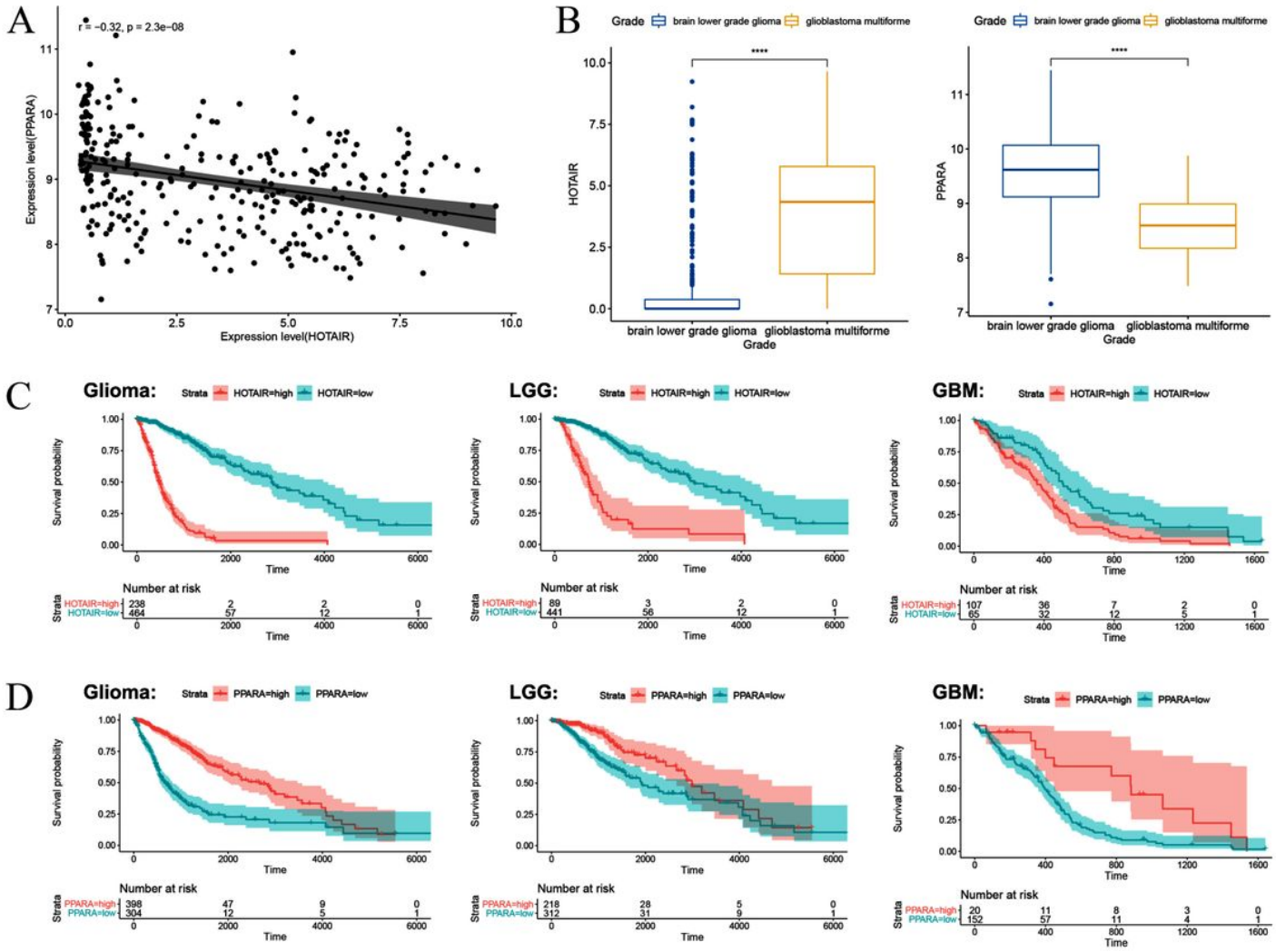

Figure 2

HOTAIR and PPARα has a significant negative correlation. Low expression of PPARα and high expression of HOTAIR predicted a poor prognosis A) Scatter plots of HOTAIR and PPARα expression. B) Box diagram of HOTAIR and PPARα expression in different grades of glioma. ****, p<0.0005. C) Survival curve plots between different HOTAIR expression groups. D) Survival curve plots between different PPARα expression groups.

Figure 2

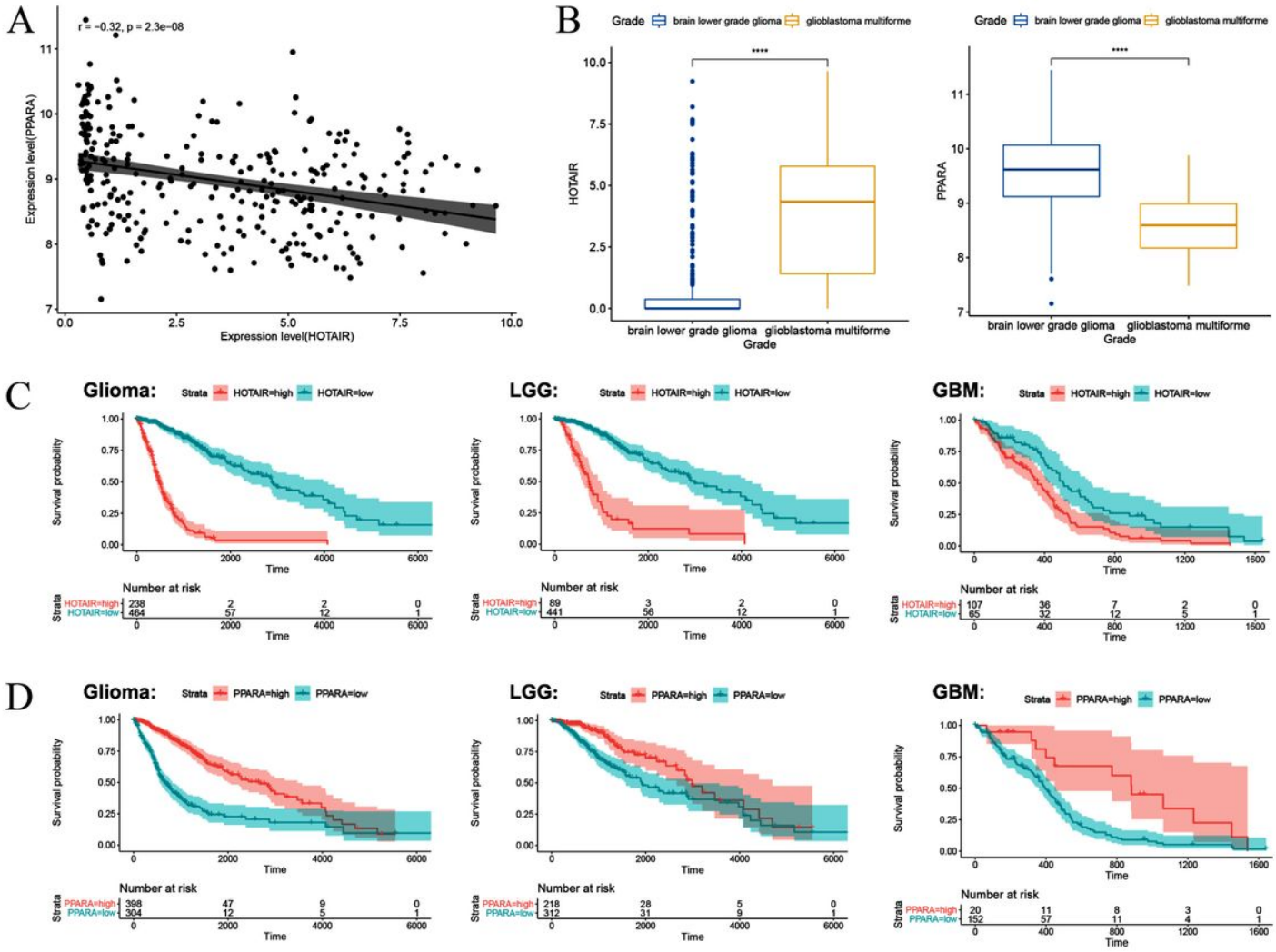

Figure 2

HOTAIR and PPARα has a significant negative correlation. Low expression of PPARα and high expression of HOTAIR predicted a poor prognosis A) Scatter plots of HOTAIR and PPARα expression. B) Box diagram of HOTAIR and PPARα expression in different grades of glioma. ****, p<0.0005. C) Survival curve plots between different HOTAIR expression groups. D) Survival curve plots between different PPARα expression groups.

Figure 2

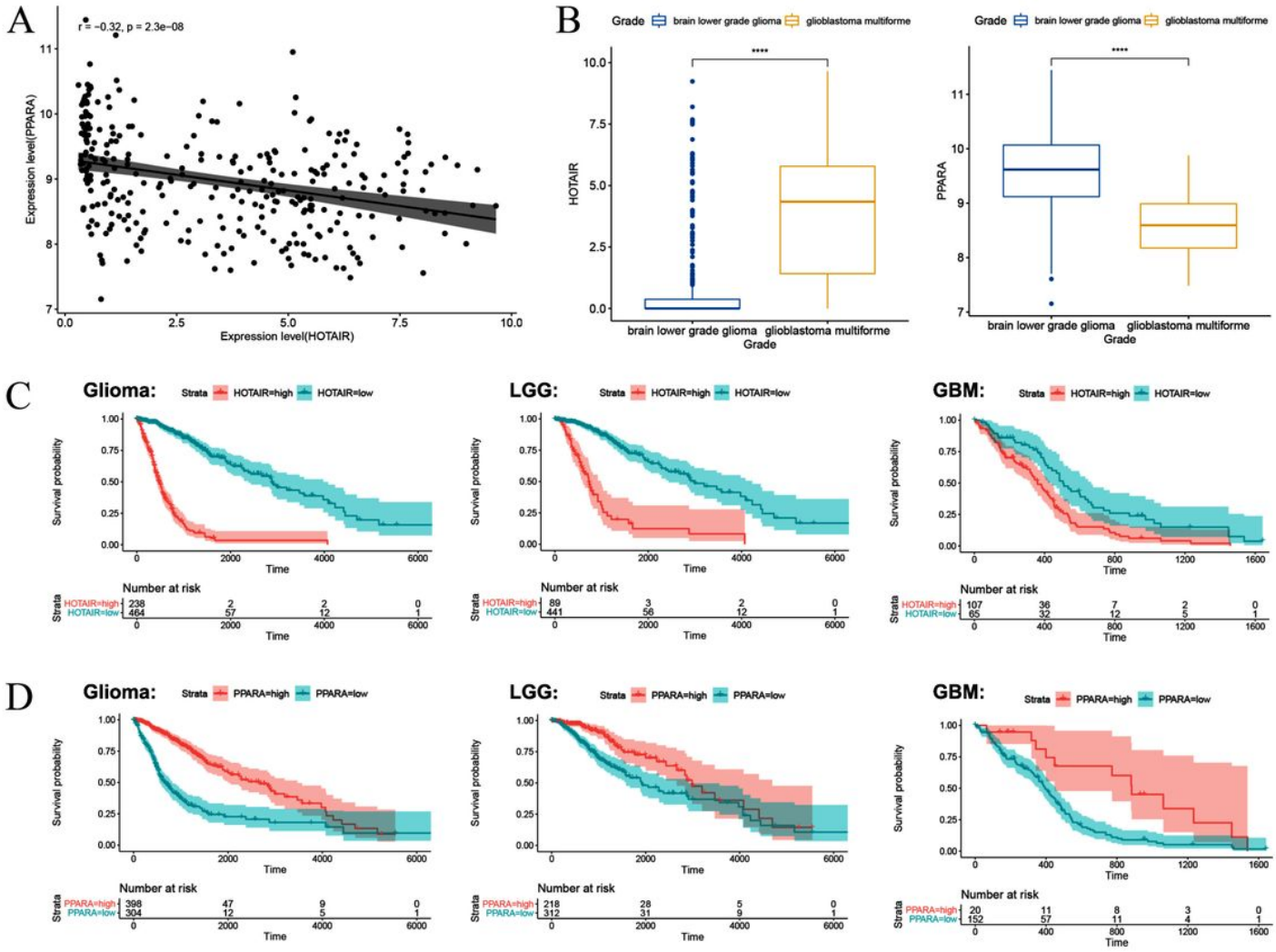

Figure 2

HOTAIR and PPARα has a significant negative correlation. Low expression of PPARα and high expression of HOTAIR predicted a poor prognosis A) Scatter plots of HOTAIR and PPARα expression. B) Box diagram of HOTAIR and PPARα expression in different grades of glioma. ****, p<0.0005. C) Survival curve plots between different HOTAIR expression groups. D) Survival curve plots between different PPARα expression groups.

Figure 3

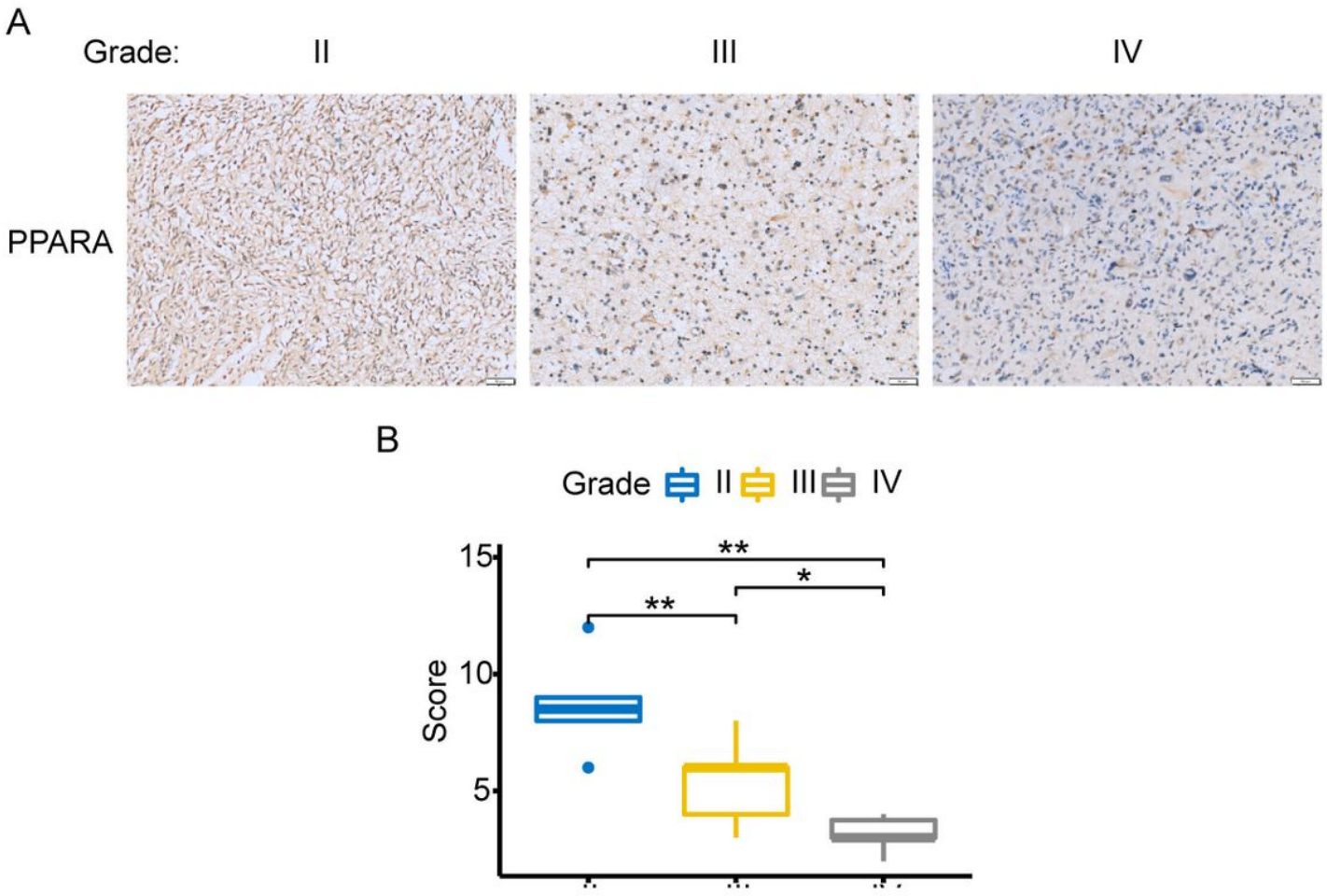

Figure 3

PPARα expression decreased in clinical samples of patients with high-grade glioma. A) PPARα immunohistochemistry staining of glioma samples of different grades. B) Statistical results of immunohistochemistry.

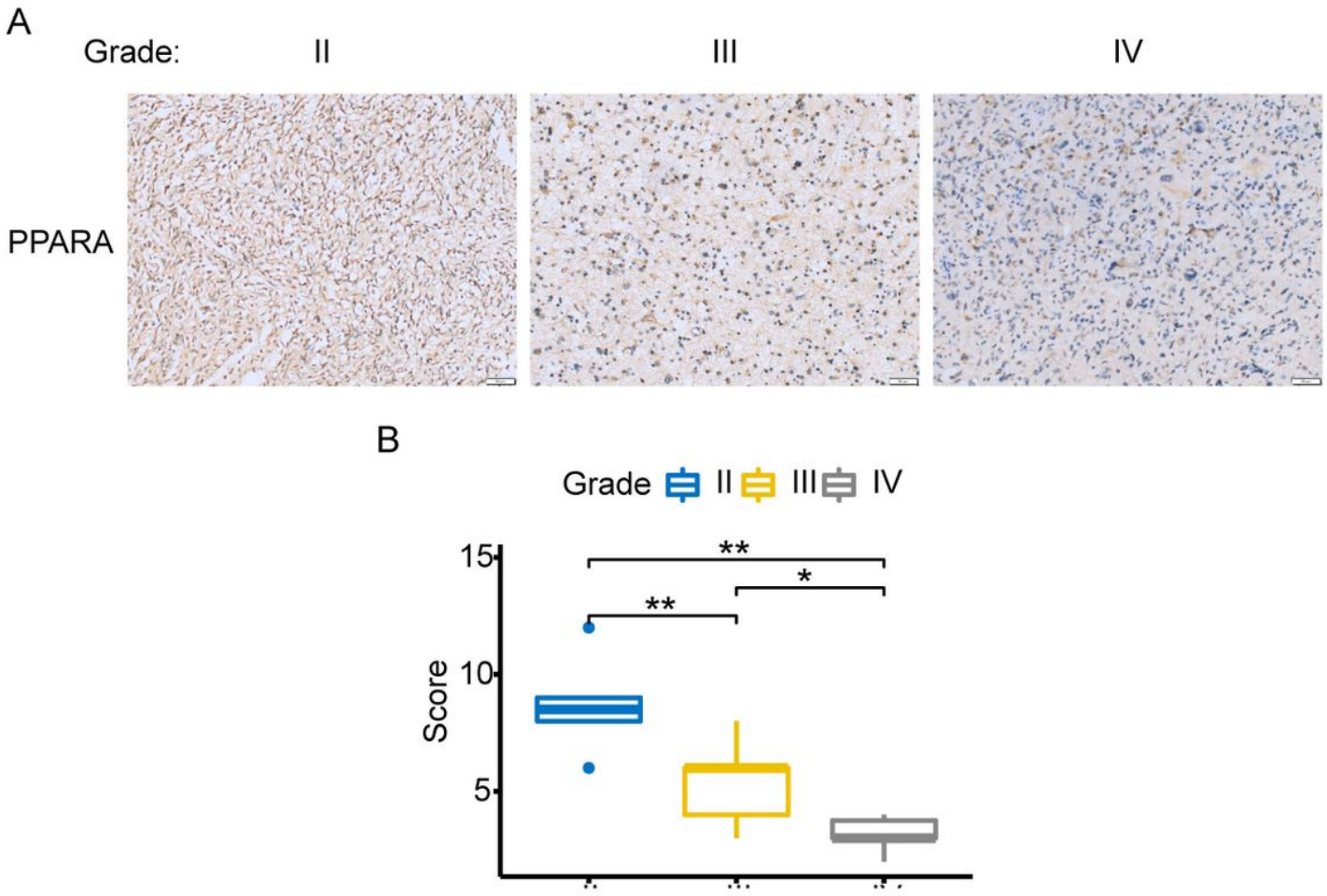

Figure 3

PPARα expression decreased in clinical samples of patients with high-grade glioma. A) PPARα immunohistochemistry staining of glioma samples of different grades. B) Statistical results of immunohistochemistry.

Figure 3

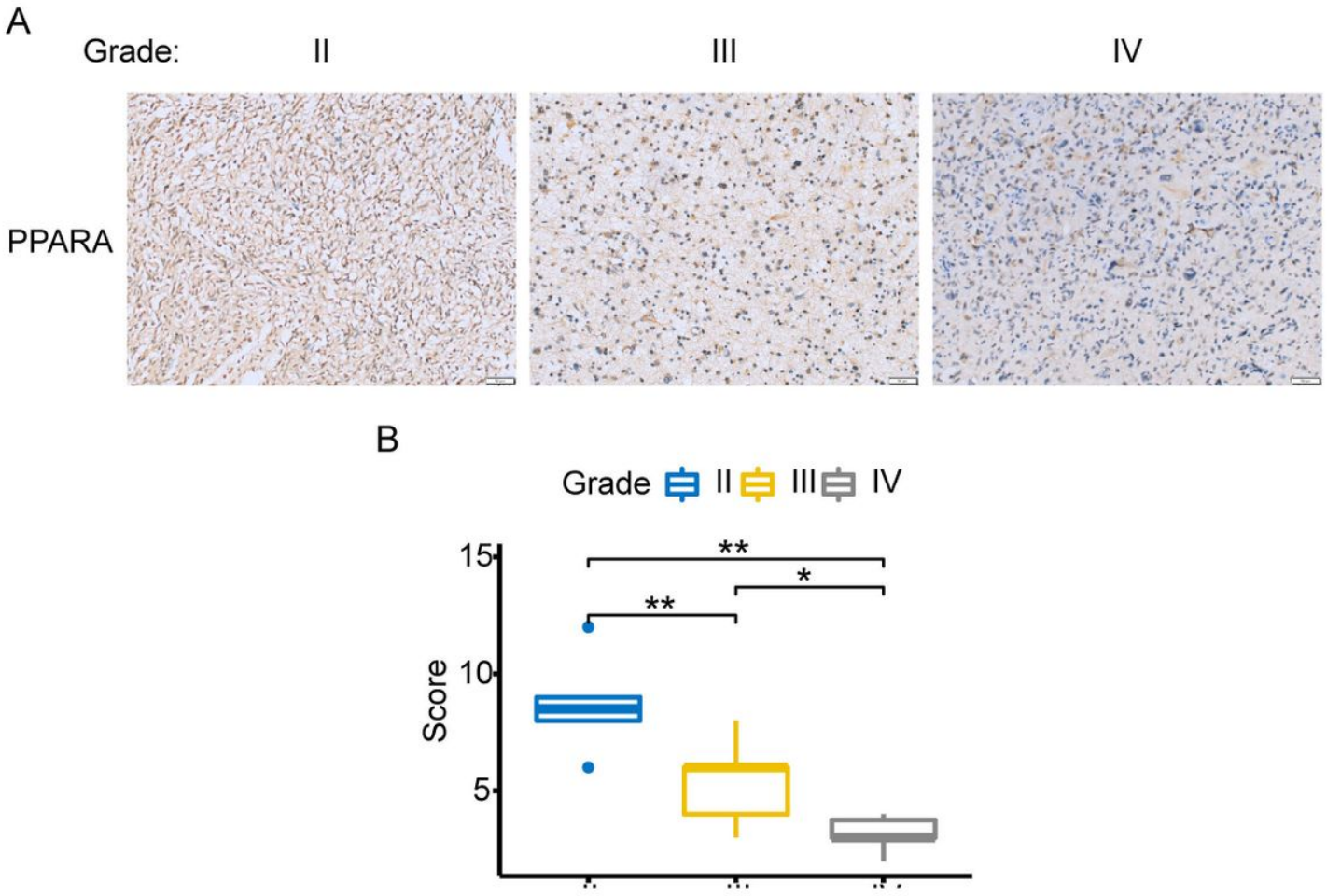

Figure 3

PPARα expression decreased in clinical samples of patients with high-grade glioma. A) PPARα immunohistochemistry staining of glioma samples of different grades. B) Statistical results of immunohistochemistry.

Figure 4

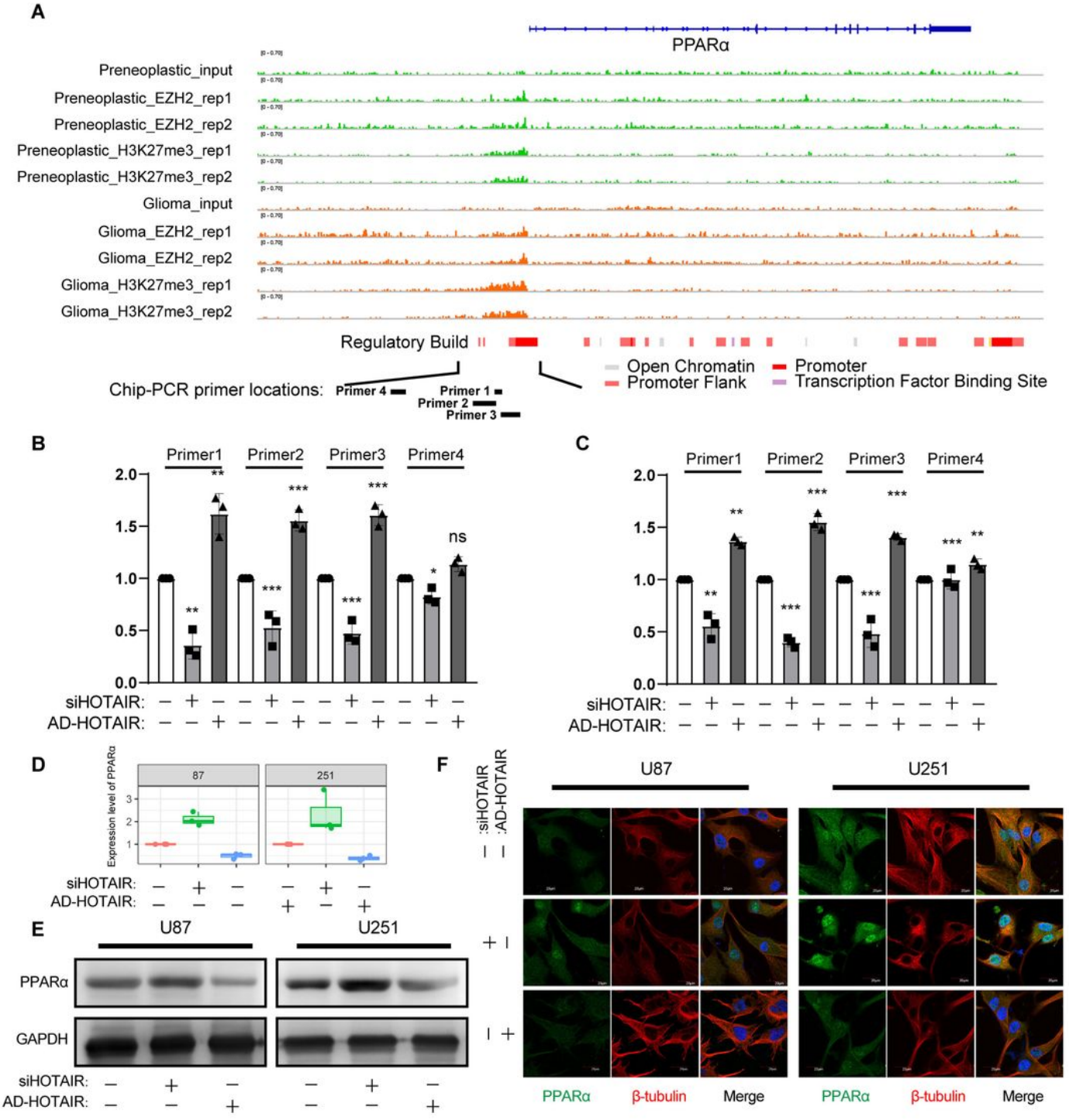

Figure 4

HOTAIR enhanced the degree of H3K27me3 binding to the PPARα promoter. A) EZH2 and H3K27me3 proteins bind to the promoter region of PPARα gene in different grades of glioma. B) ChIP analysis of the H3K27me3 protein in the promoter region of PPARα gene in different treatment groups in U87 cell line. C) ChIP analysis of the H3K27me3 protein in the promoter region of PPARα gene in different treatment

groups in U251 cell line. D) Quantitative PCR analysis. E) Western blot. F) Immunofluorescence. Bar, 20 μm.

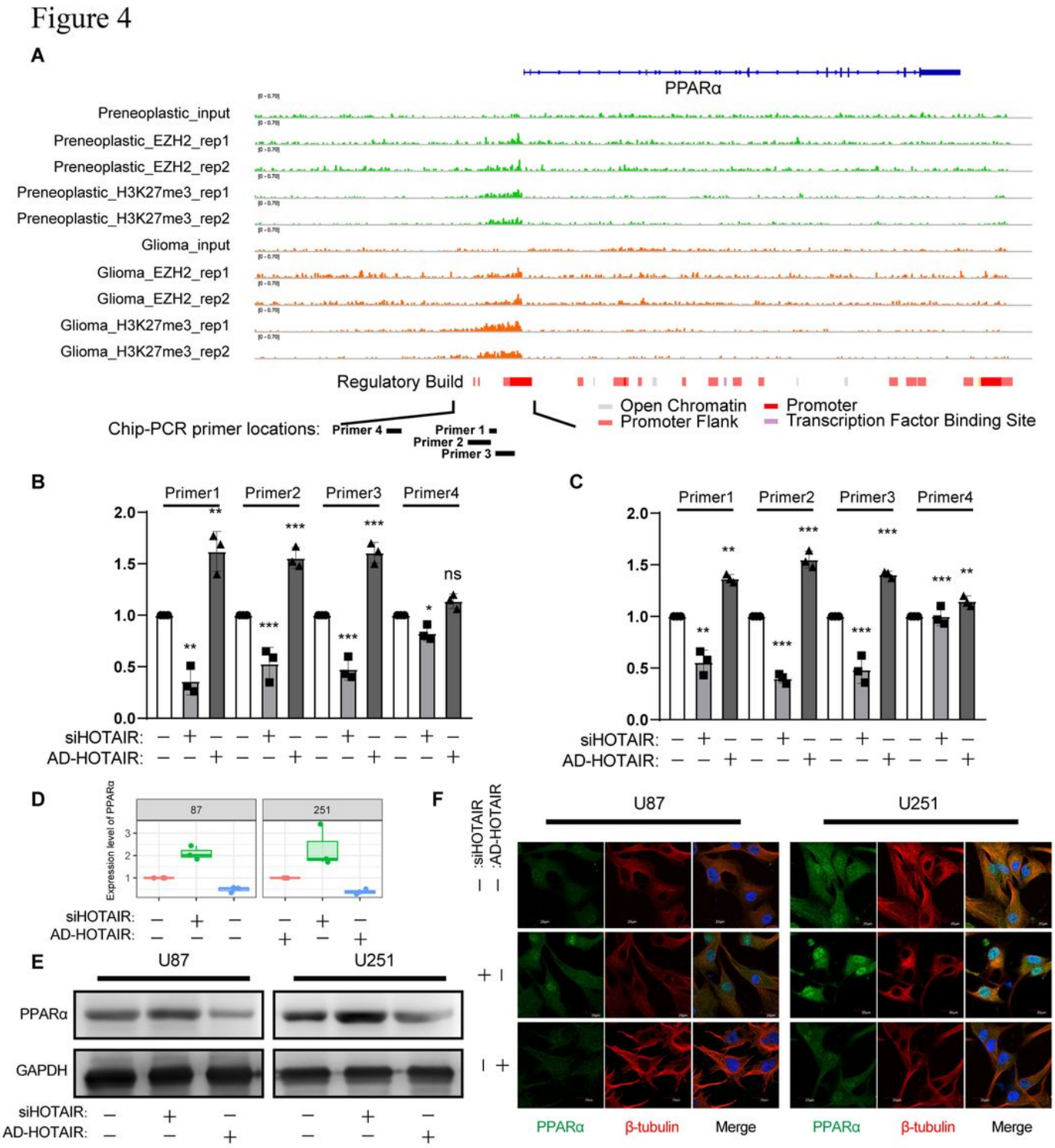

Figure 4

HOTAIR enhanced the degree of H3K27me3 binding to the PPARα promoter. A) EZH2 and H3K27me3 proteins bind to the promoter region of PPARα gene in different grades of glioma. B) ChIP analysis of the H3K27me3 protein in the promoter region of PPARα gene in different treatment groups in U87 cell line. C)

ChIP analysis of the H3K27me3 protein in the promoter region of PPARα gene in different treatment groups in U251 cell line. D) Quantitative PCR analysis. E) Western blot. F) Immunofluorescence. Bar, 20 μm.

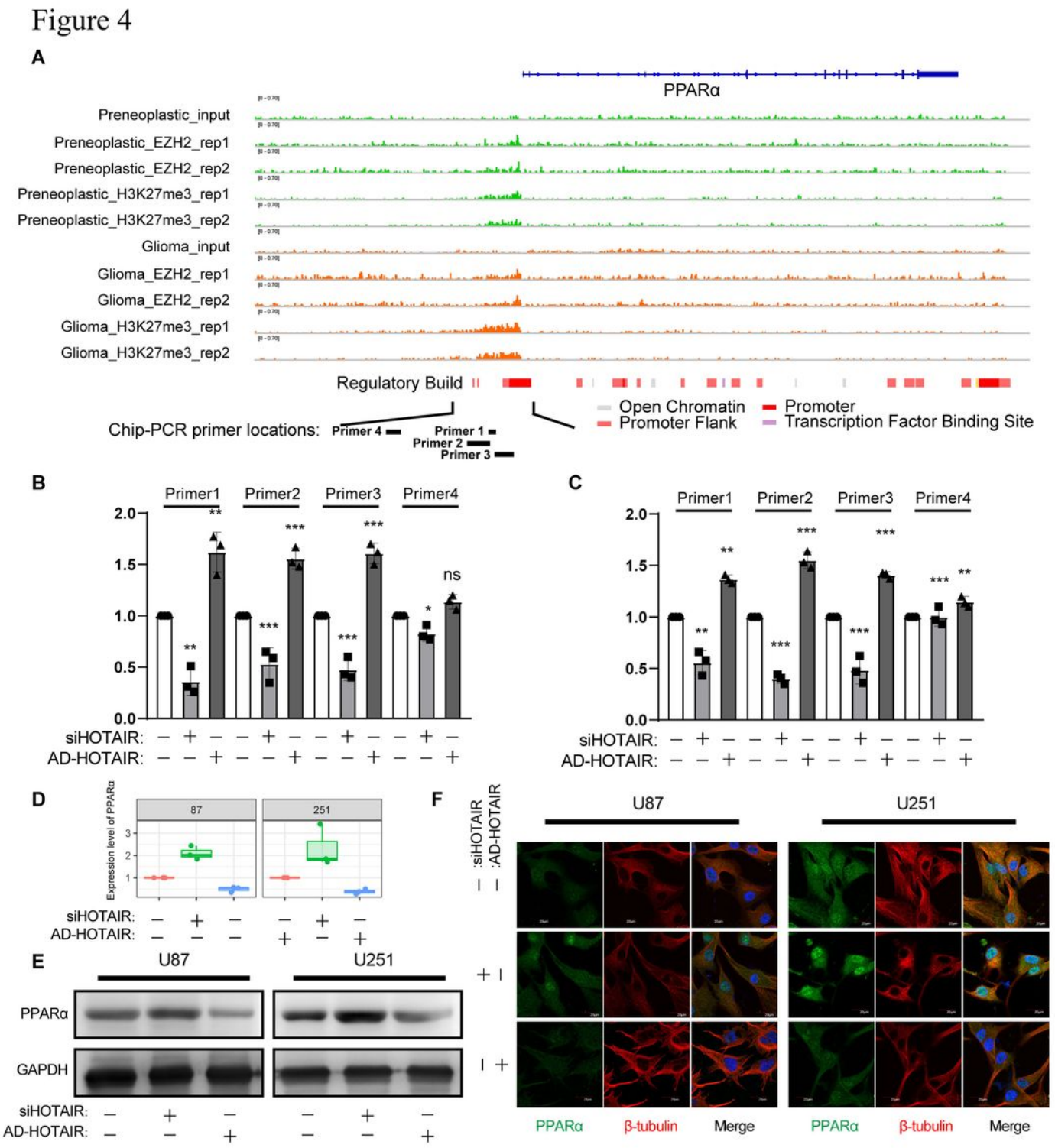

Figure 4

HOTAIR enhanced the degree of H3K27me3 binding to the PPARα promoter. A) EZH2 and H3K27me3 proteins bind to the promoter region of PPARα gene in different grades of glioma. B) ChIP analysis of the

H3K27me3 protein in the promoter region of PPARα gene in different treatment groups in U87 cell line. C) ChIP analysis of the H3K27me3 protein in the promoter region of PPARα gene in different treatment groups in U251 cell line. D) Quantitative PCR analysis. E) Western blot. F) Immunofluorescence. Bar, 20 μm.

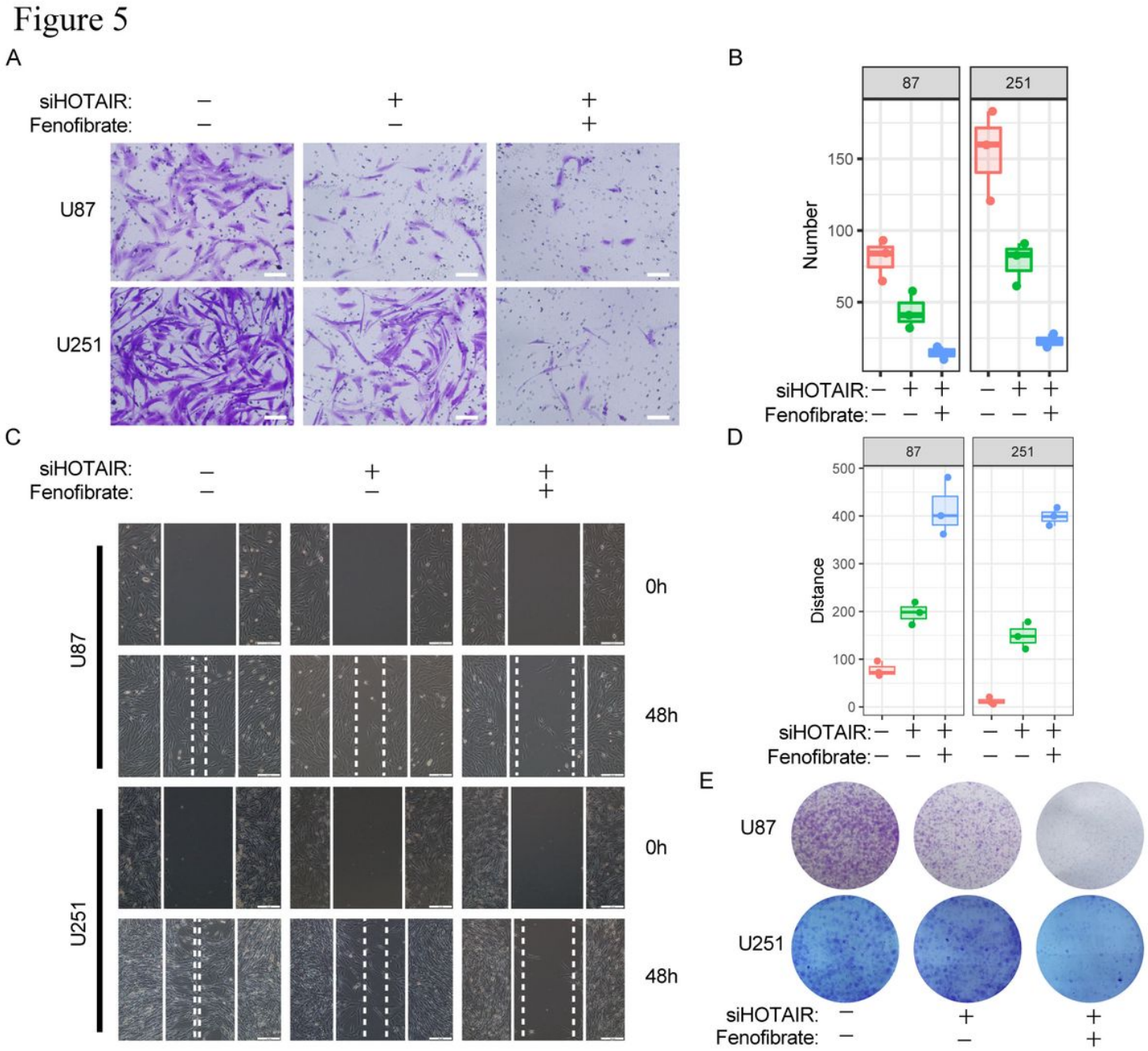

Figure 5

Si-HOTAIR and fenofibrate combined therapy attenuated the migration and colony formation abilities of U87 and U251 glioma cells. (A) Transwell analysis. White bar, 200 μm. (B) Statistical analysis of the transwell assay. (C) Wound-healing assay. White bar, 200 μm. (D) Colony formation assay. (E) Statistical analysis of the colony formation assay.

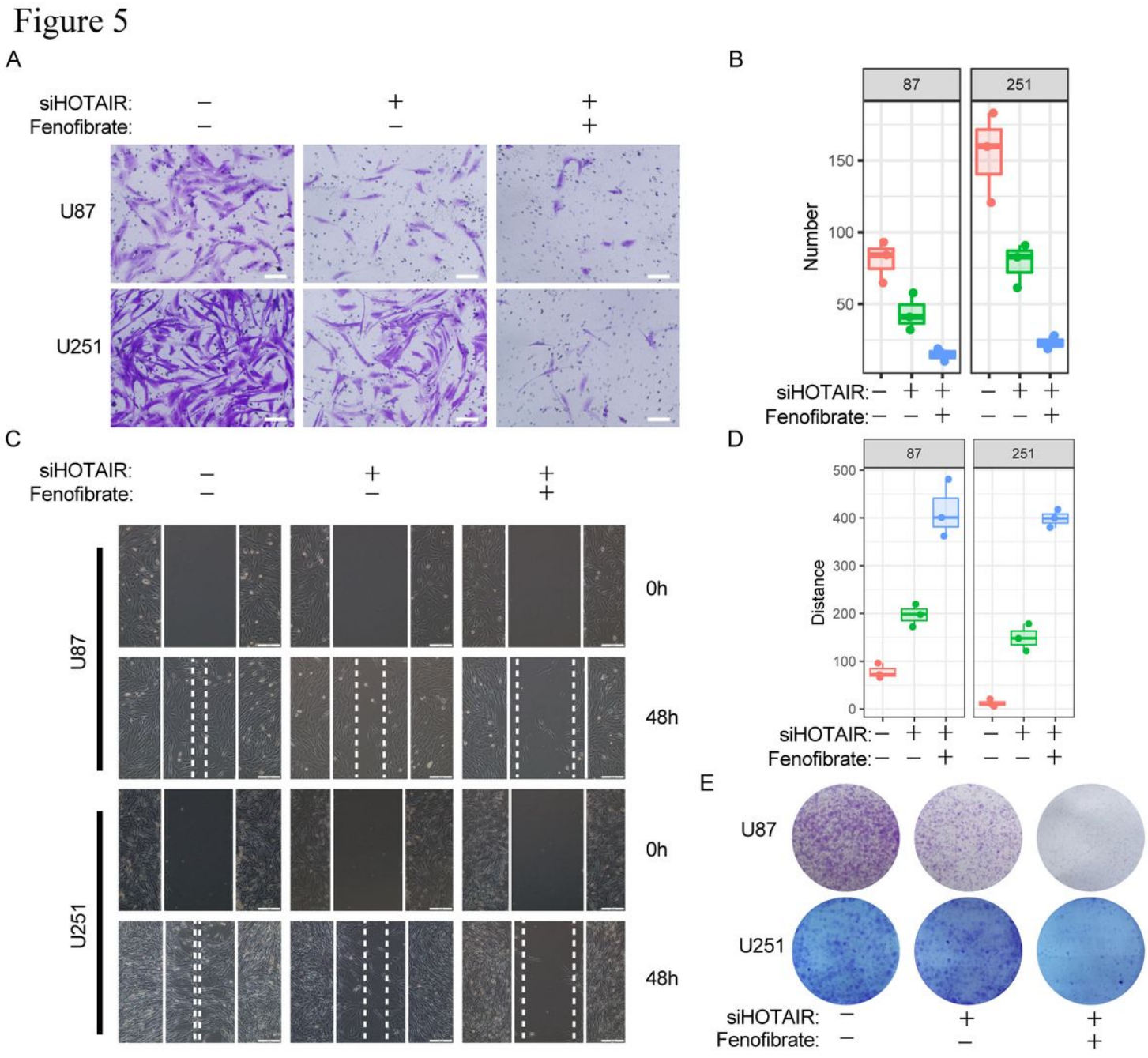

Figure 5

Si-HOTAIR and fenofibrate combined therapy attenuated the migration and colony formation abilities of U87 and U251 glioma cells. (A) Transwell analysis. White bar, 200 μm. (B) Statistical analysis of the transwell assay. (C) Wound-healing assay. White bar, 200 μm. (D) Colony formation assay. (E) Statistical analysis of the colony formation assay.

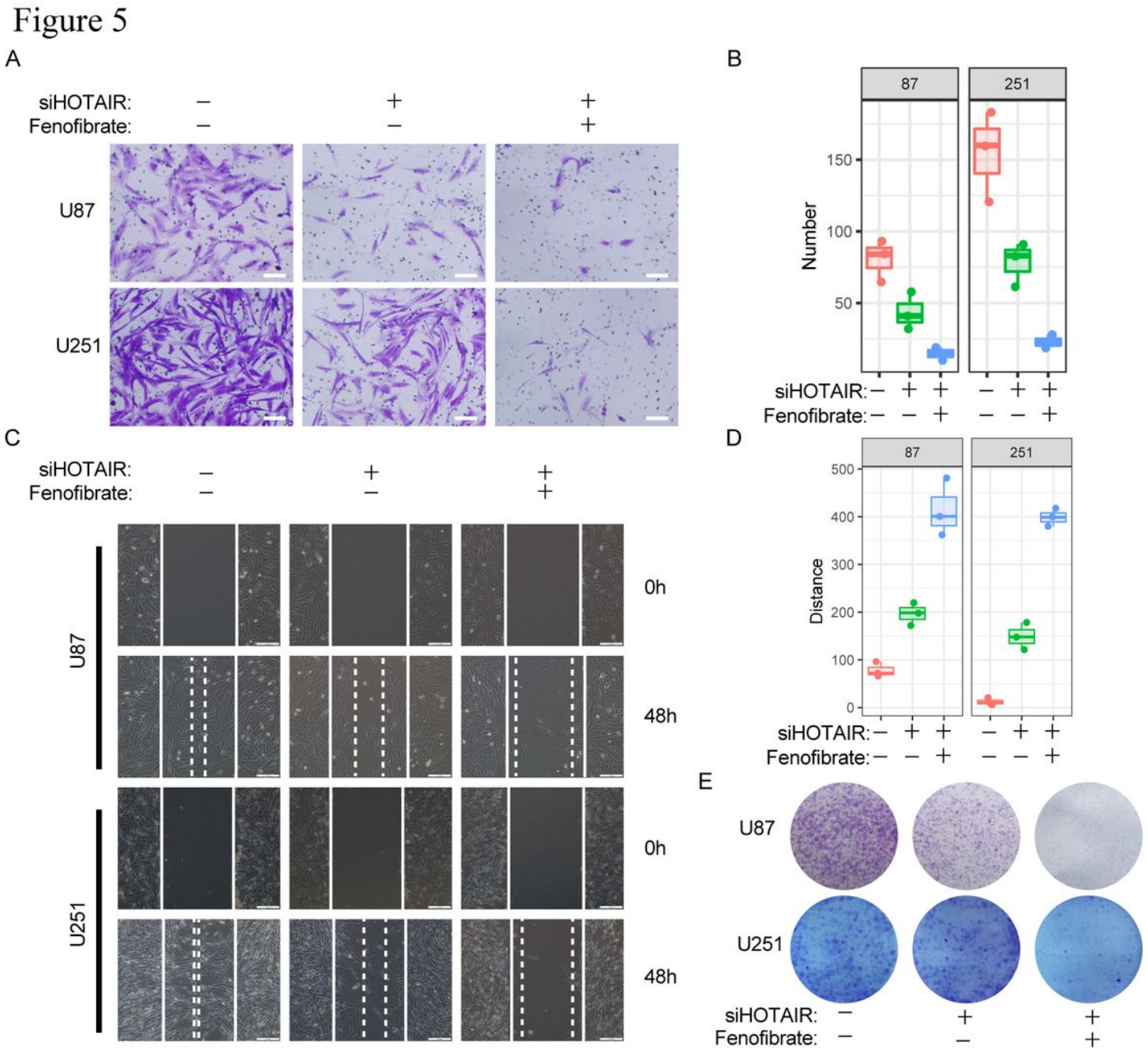

Figure 5

Si-HOTAIR and fenofibrate combined therapy attenuated the migration and colony formation abilities of U87 and U251 glioma cells. (A) Transwell analysis. White bar, 200 μm. (B) Statistical analysis of the transwell assay. (C) Wound-healing assay. White bar, 200 μm. (D) Colony formation assay. (E) Statistical analysis of the colony formation assay.

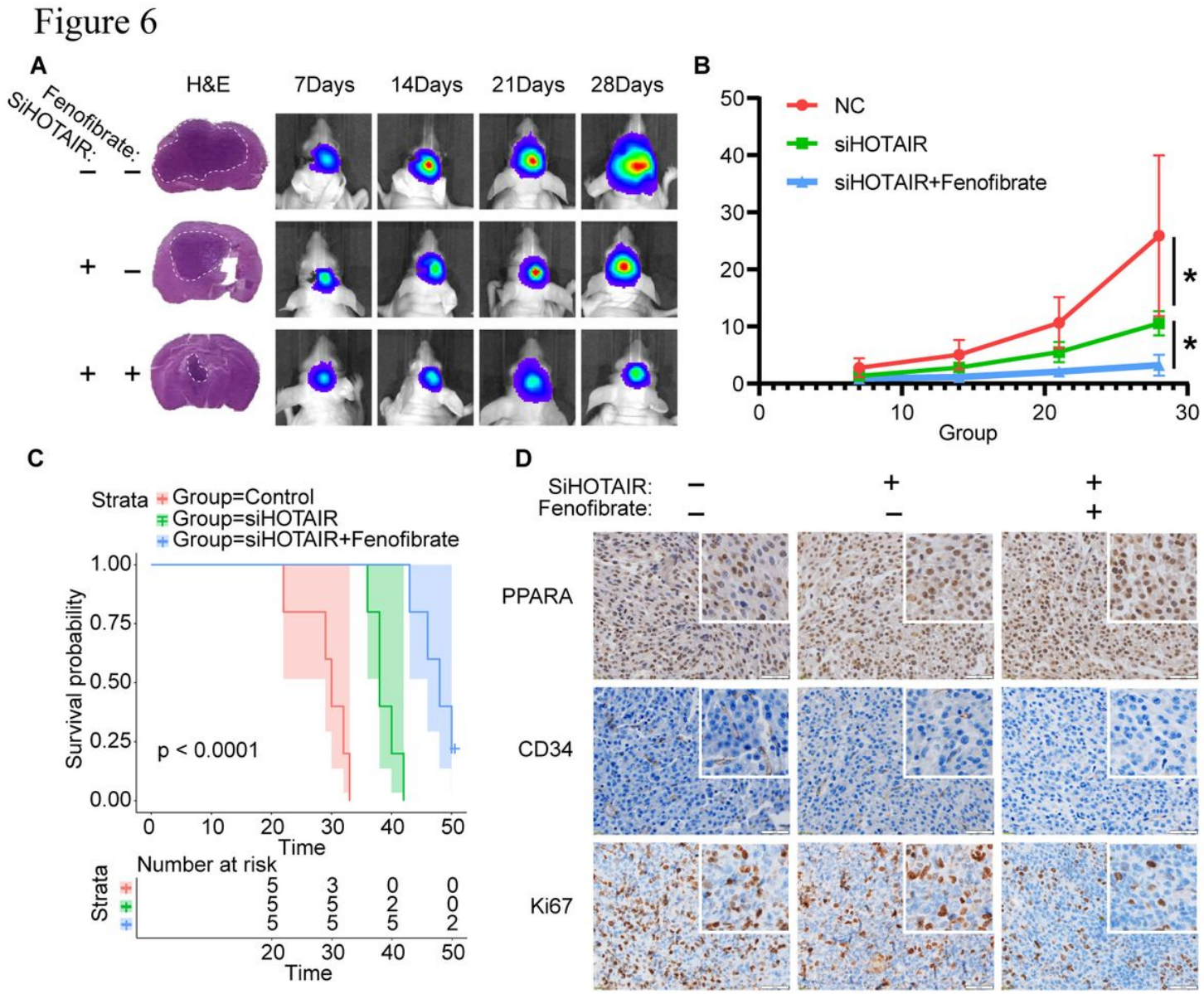

Figure 6

Si-HOTAIR and fenofibrate combined therapy can slow glioma growth. (A) H&E staining of different groups of U87 intracranial glioma models. Tumor volume was measured every seven days by in vivo imaging. (B) Statistical analysis results of the control and combined therapy intracranial glioma groups every seven days. (C) Survival curve plots of control and combined therapy intracranial glioma groups. D) Immunohistochemistry staining. White bar, 50 μm.

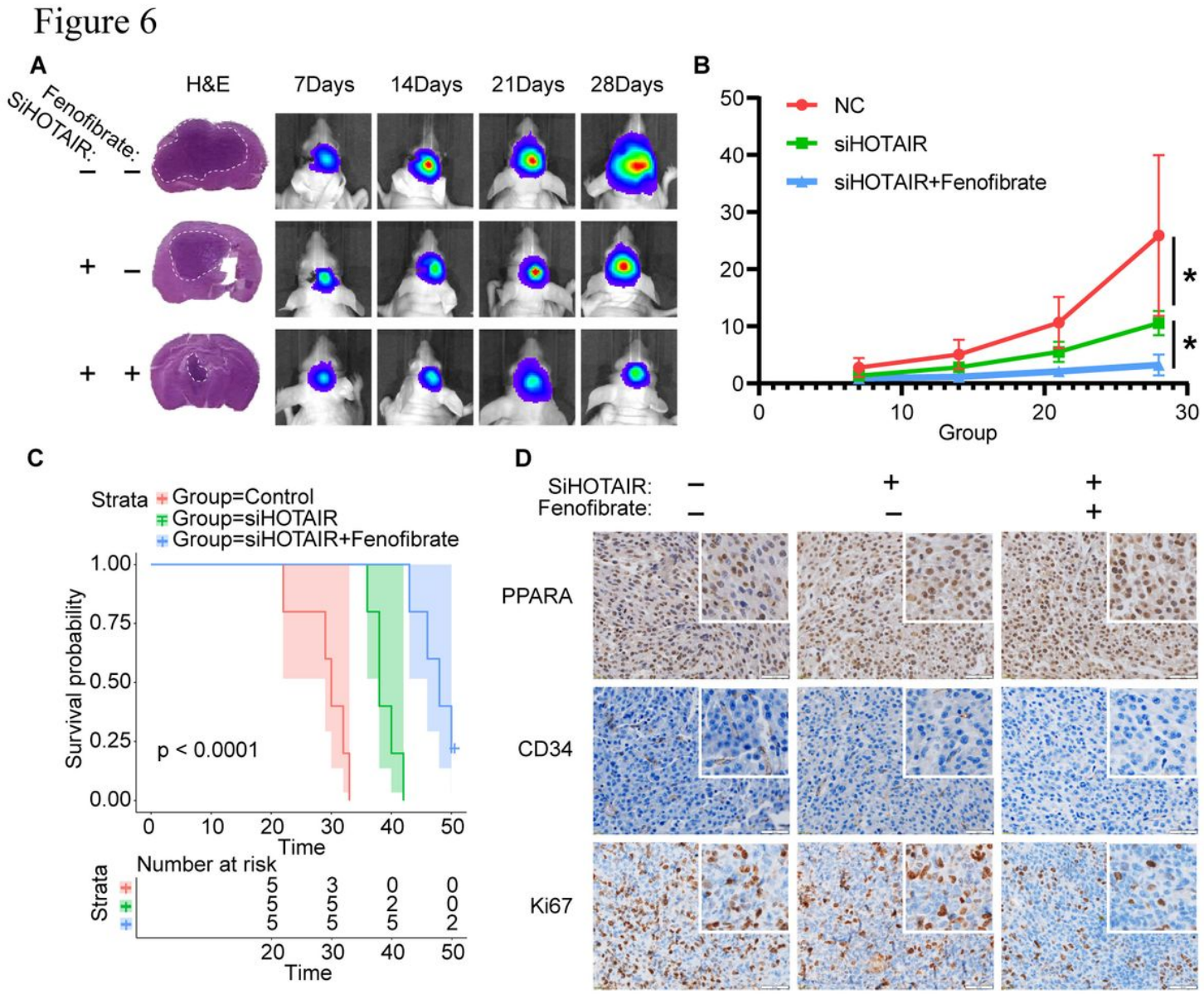

Figure 6

Si-HOTAIR and fenofibrate combined therapy can slow glioma growth. (A) H&E staining of different groups of U87 intracranial glioma models. Tumor volume was measured every seven days by in vivo imaging. (B) Statistical analysis results of the control and combined therapy intracranial glioma groups every seven days. (C) Survival curve plots of control and combined therapy intracranial glioma groups. D) Immunohistochemistry staining. White bar, 50 μm.

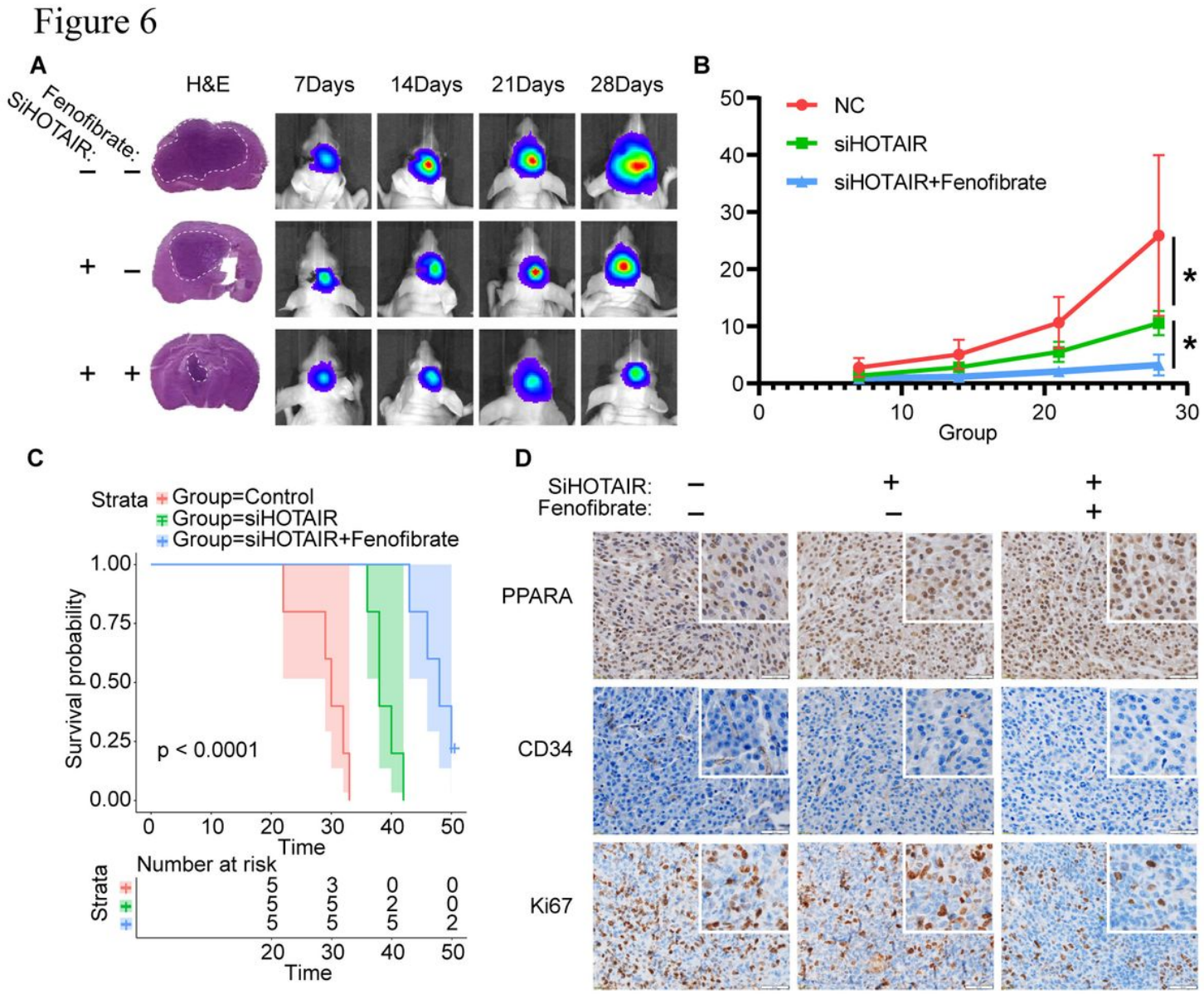

Figure 6

Si-HOTAIR and fenofibrate combined therapy can slow glioma growth. (A) H&E staining of different groups of U87 intracranial glioma models. Tumor volume was measured every seven days by in vivo imaging. (B) Statistical analysis results of the control and combined therapy intracranial glioma groups every seven days. (C) Survival curve plots of control and combined therapy intracranial glioma groups. D) Immunohistochemistry staining. White bar, 50 μm.

Supplementary Files

This is a list of supplementary files associated with this preprint. Click to download.

- Supplementarymaterial.docx

- Supplementarymaterial.docx
- Supplementarymaterial.docx
- SupplementaryTable1.xlsx
- SupplementaryTable1.xlsx
- SupplementaryTable1.xlsx